**How to cite:** Taşar, B., Üneş, F., Gemici, E., Demirci, M., Kaya, Y.Z. (2023) Numerical Modeling of Submerged Vane Flow. *2023 "Air And Water – Components of the Environment" Conference Proceedings*, Cluj-Napoca, Romania, p. 111-120, DOI: 10.24193/AWC2023_11.

# NUMERICAL MODELING OF SUBMERGED VANE FLOW

***Bestami TAŞAR [1], Fatih ÜNEŞ[1]*, Ercan GEMİCİ [2], Mustafa DEMİRCİ[1], Yunus Ziya KAYA[3]***

**DOI: 10.24193/AWC2023_11**

**ABSTRACT.** Scours in rivers occur due to high flow velocities. In order to reduce scour, flow velocities need to be reduced. Submerged vane structures are effective in both reducing the flow rate and directing the flow. In this study, numerical modeling was made with submerged vane structures. Models of the measured flow velocities in the channel, where submerged vane experiments were performed before, were compared with the results of the submerged vane experiment by using the 3-dimensional computational fluid dynamics (CFD) method. In the present CFD model, continuity and momentum, turbulence model equations are applied. For the turbulence viscosity, k-ε turbulence model is used. The results of the present model are compared with the previous experimental work.

## 1. INTRODUCTION

Rivers carry sediments caused by erosion and scouring in the streambed. As a consequence of erosions in the bed, scouring occurs, the materials carried are transported up to where they can be transported depending on the drag force, and accumulation occurs with bed sedimentation in places that cannot be transported. As a result of this erosion and accumulation: the stream morphology changes, the structures on the stream may be affected or the quality of the stream may deteriorate.

Studies conducted with a submerged vane in meander curves in the 1980s by Odgaard and Kennedy (1982), Odgaard and Kennedy (1983), Odgaard and Lee (1984) and Odgaard and Mosconi (1987) pioneered the entry of submerged vane into the literature as a new method. Marelius and Sinha (1998) conducted a study to create the optimum vane angle required to create the strongest secondary circulation in the open channel flow. They analyzed the results of four different approach angles of 25°, 36°, 45° and 57° to obtain an approximate estimate of the optimum vane angle. Ghorbani and Kells (2008) examined the effect of a submerged vane on local scour in a cylindrical leg. For this purpose, they evaluated various vane heights, orientation angles and flow depths, all for a fixed Froude

[1] Iskenderun Technical University, Hatay – TURKEY, e-mail: bestami.tasar@iste.edu.tr fatih.unes@iste.edu.tr *(corresponding author), mustafa.demirci@iste.edu.tr

[2] Bartin University, Bartin – TURKEY, e-mail: egemici@bartin.edu.tr

[3] Osmaniye Korkut Ata University, Osmaniye – TURKEY, e-mail: yunuszkaya@osmaniye.edu.tr

number. Davoodi and Bejestan (2012) tested four different longitudinal distances between submerged vane, equal to 4H, 6H, 8H and 10H, under four different flow conditions. The Froude number was used at flows of 0,45, 0,55 and 0,60 and 0,66, respectively. The results of their study showed that submerged vane can change flow patterns upstream of the inlet if the amount of inlet sediment is reduced by up to 31%. Fathi and Zomorodian (2018) present the results of laboratory experiments investigating how submerged vanes affect scrubbing around a vertical wall and overflow abutments under clean water conditions. Kalathil et al. (2018) used submerged vanes to control sediment entry into the inlet channel with a physical model. The vane angle, the number of vane rows and vane spacing were examined in terms of different mean flow depths. Lake et al. (2021) investigated the effect of river-based, submerged vane structures in Australia. Studies conducted cannot fully explain to what extent which feature affects the performance of the submerged vane. River meandering regulation and especially submerged vane studies; the complexity of the subject matter is unsteady and nonlinear due to the effect of more parameters on the event and has been studied by very few researchers in the past. Therefore, there is very limited study.

In this study, experiments at the open channel laboratory were performed on the meandering part with a single array with 6 submerged vane ($V_1$) and without submerged vane ($V_0$). The experimental results of the flow velocities measured in the open channel flow at the meander were confirmed by CFD simulations for $V_0$ and $V_1$ situations. CFD models are verified by Open channel experiments in no vane ($V_0$) and single array with 6 submerged vanes ($V_1$) situations.

## 2. MATERIAL AND METHODS

The performance of $V_0$ and $V_1$ situations in meandering open channel flows has been investigated by using a flow rate of 10 L/s in this study. Detailed information about the experimental setup, experimental conditions and numerical model for the $V_0$ and $V_1$ situations conducted in the open channel are given below.

### 2.1. Experimental Study

In the laboratory, a 30 cm wide curvilinear canal was built within a 50 cm wide rectangular channel within the existing open channel system. Hydraulic parameters belonging to the submerged vane experiments performed for the Q: 10 L/s streamflow is given in Table 1. In Table 1, “Q” channel flow rate; “B” is the channel width; “d” Depth of flow; “A” wetted area; "T” wetted perimeter; “$R_h$” Hydraulic radius; “$V_{mean}$” means Inlet average flow velocity and “Fr” Flow Froude number (river regime / flood regime). In this study, since the Froude number is less than 1, it was observed that there is a subcritical flow or river regime. Here, the Fr number was found to be less than 1 in the open channel experimental setup, since the place where the flow velocity is measured is close to the channel entrance.

*Table 1. The flow conditions for experiment*

| $Q$ (L/s) | $B$ (m) | $d$ (m) | $A$ (m$^2$) | $T$ (m) | $R_h$ (m) | $V_{mean}$ (m.s$^{-1}$) | $Fr$ |
|---|---|---|---|---|---|---|---|
| 0,010 | 0,300 | 0,055 | 0,017 | 0,410 | 0,042 | 0,59 | 0,92 |

In order to reduce the turbulence of the flow entering the canal, the energy of the water was reduced by taking the water entering with the pump into the settling tank. The open channel assembly in which the submerged vane experiment was performed had a base slope of 0,0003. A meandering channel, approximately 3 meters long and 30 cm wide, was constructed along the 50 * 50 sectioned rectangular channel. A strongly curved 30° meander is connected to the upstream and downstream channels. The curvature has a center radius $R$ = 3,60 m. The experimental setup is shown in Fig. 1.

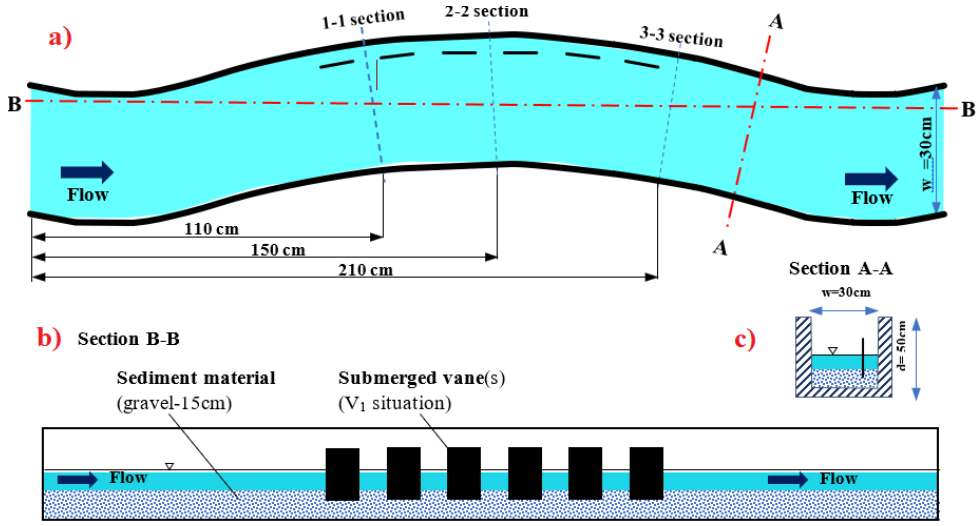


**Fig. 1.** ***Submerged vane experimental set-up for $V_1$ situation: a) Channel top (plan) view, b) Cross section view, c) Section view***

The flow discharges were measured by an Acoustic Doppler Velocimetry (ADV) flowmeter. Measurements were made at 60% (0.6d) of the depth. Considering the single 6-vane sequence, measurements were taken in the middle of the 10 cm gap (5 cm) after each vane. Flow velocity measurements were taken perpendicular to the flow at 2.5 cm intervals at 8 post-vane measurement points. The section measured after the vane in the first row was called the 1-1 section. The section after the 3th vane was called the 2-2 section. For the case of $V_1$, the view at 16 (8 points x 2 sections) points after the vane is measured is given in Fig. 2 below.

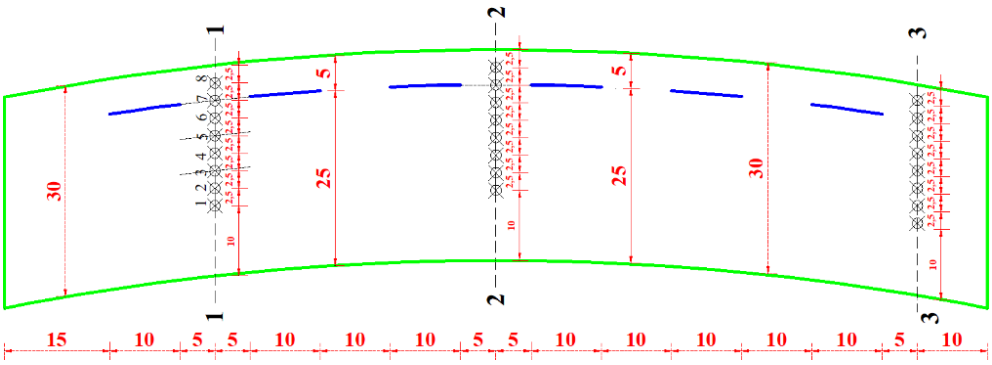


**Fig. 2.** ***According to $V_1$ situation, all sections and points which measured in the channel***

When Fig. 2 is examined, it is aimed to investigate the effect after the vane as a reference in cases with and without a vane. In each cross-section, the flow velocity changes at 2,5 cm intervals were examined by comparing the $V_0$ and $V_1$ situations.

## 2.2. Numerical (CFD) model

The studied flow is an open-channel flow. Flows in the open channel are high velocities and turbulent. According to the literature, the standard k-ε turbulence model can be used in the 3d numerical modeling of the flow(Hirt & Nichols, 1981). The investigated open channel flow is a 3D, turbulent, steady free surface flow. Equations used in the numerical model; continuity, momentum, and turbulence equations. The standard k-e turbulence equation was used as the turbulence equation. In this study, the volume of fluid (VOF) method was used to calculate the water-air interface. The VOF method essentially determines whether the element volumes in the computational mesh are empty, partially filled, or completely filled with water. (Hirt & Nichols, 1981)

Approximately 1.5-2 million meshes were used in the designs. 1886245 mesh for $V_0$ submerged vane case and for the $V_1$ submerged vane case 1618735 meshes are assigned. Also, tetrahedron-type meshes were used in the design. Details of the meshing design are given in Fig. 3. The 3-dimensional (3D) analysis was built up for $V_0$ and $V_1$ submerged vane structures. The 3D model was created according to the open channel experiment setup consisting of 1 main bend channel (Fig. 4.). According to the experimental inlet measure (Table 1), initial conditions, and boundary layer conditions are established and will be compared with the experimental results. Fig. 4a and 4b show the surfaces for the CFD model solution. According to the water inlet height accepted, the "velocity inlet" region, submerged vane-open channel surfaces "wall" surfaces and downstream side outlet section "outflow" are considered in the model (Fig. 4a-b). In the case of flow of 10 L/s, for CFD analysis, the water inlet height was defined as 5,5 cm. The full implicit scheme was used in the model(Unes and Varcin 2017).

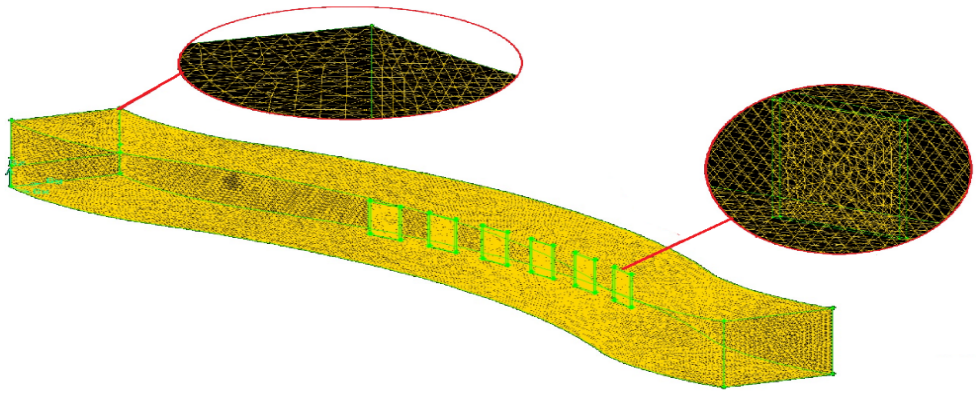

**Fig. 3.** ***Channel and submerged vane meshing for $V_1$ model***

The time step for the turbulence model used as 0,1 second and a solution was made for 600 seconds, during which the numerical solution became stable. The numerical solution of the fundamental equations according to the boundary conditions was made using the Ansys-Fluent program based on the finite volume method (Ansys).

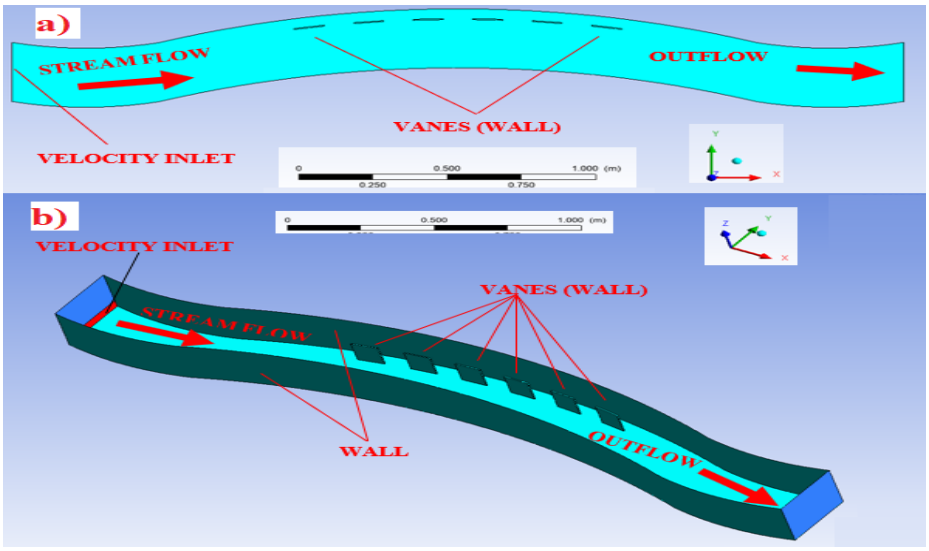


**Fig. 4.** ***Boundary conditions for $V_1$ situation: a) top view; b) downstream view)***

## 3. RESULTS AND DISCUSSIONS

In Table 2 and Fig. 9, CFD results are given with the measured test points according to the 1-1 and 2-2 sections. Considering the 0,0,0 (x,y,z) starting point; 1,1 meters is accepted as a 1-1 section, 1,5 meters is accepted as a 2-2 section and the distance between the measurement points is 2,5 cm.

In the Fig. 5, the dimensionless velocity is "$u/u_{mean}$"; The 1st point represents the point close to the inner bank, and the 8th point represents the point close to the outer bank. The experimental and numerical model velocity values obtained in Section 1-1 are shown in Table 2 and Fig. 5. Table 2 shows the error rates by comparing the experimental and CFD analysis results.

***Table 2. CFD and experimental results for $V_0$ and $V_1$ situations at Sections 1-1 and 2-2***

| Vane situation | Section No | Point No | Experimental dimensionless flow velocity results | CFD dimensionless flow velocity results | Error (%) |
|---|---|---|---|---|---|
| $V_0$ | 1-1 | 1 | 0,962 | 0,961 | 0,14 |
| | | 2 | 1,001 | 0,965 | 3,64 |
| | | 3 | 0,997 | 0,973 | 2,44 |
| | | 4 | 0,993 | 0,971 | 2,22 |
| | | 5 | 1,008 | 0,985 | 2,25 |
| | | 6 | 1,012 | 1,003 | 0,89 |
| | | 7 | 1,002 | 1,053 | 5,09 |
| | | 8 | 1,026 | 1,090 | 6,33 |
| $V_0$ | 2-2 | 1 | 1,097 | 0,970 | 11,60 |
| | | 2 | 1,112 | 0,977 | 12,13 |
| | | 3 | 1,015 | 0,977 | 3,67 |
| | | 4 | 0,917 | 0,975 | 6,28 |
| | | 5 | 0,954 | 0,985 | 3,19 |
| | | 6 | 0,928 | 1,007 | 8,55 |
| | | 7 | 0,961 | 1,045 | 8,71 |
| | | 8 | 1,016 | 1,064 | 4,77 |
| $V_1$ | 1-1 | 1 | 1,084 | 1,031 | 4,91 |
| | | 2 | 1,119 | 1,028 | 8,11 |
| | | 3 | 0,996 | 1,030 | 3,48 |
| | | 4 | 0,996 | 1,015 | 1,90 |
| | | 5 | 0,990 | 1,013 | 2,30 |
| | | 6 | 0,936 | 0,989 | 5,64 |
| | | 7 | 0,887 | 0,837 | 5,64 |
| | | 8 | 0,993 | 1,058 | 6,54 |
| $V_1$ | 2-2 | 1 | 1,172 | 1,062 | 9,37 |
| | | 2 | 1,183 | 1,060 | 10,43 |
| | | 3 | 1,013 | 1,060 | 4,61 |
| | | 4 | 1,013 | 1,039 | 2,59 |
| | | 5 | 0,934 | 1,025 | 9,72 |
| | | 6 | 0,912 | 0,948 | 4,02 |
| | | 7 | 0,783 | 0,742 | 5,14 |
| | | 8 | 0,991 | 1,064 | 7,38 |

When the table and graph are examined, it is seen that the error percentage of the velocities is less at the midpoints than at the edges. Maximum error was observed in

the outer bank (7-8th points) for $V_0$ situation 1-1 section (5-6%). In general, it has been found that the test and CFD results are in good agreement. In Fig. 6a-6d, velocity contours of the 1-1 and 2-2 sections are given, respectively.

According to Fig. 5a and 5b, it is seen that the velocity increases in the outer bank and decreases in the inner bank. Also, as can be seen in Fig. 6a and 6b, the flow water depth decreases in the inner bank, while the water depth increases in the outer bank (the water depth changes with the blue contour lines). Maximum error was observed in the inner bank (1-2nd points) for $V_0$ situation 2-2 section (11-12%). In general, it has been found that the experimental and CFD results are in good agreement in the $V_0$ situation.

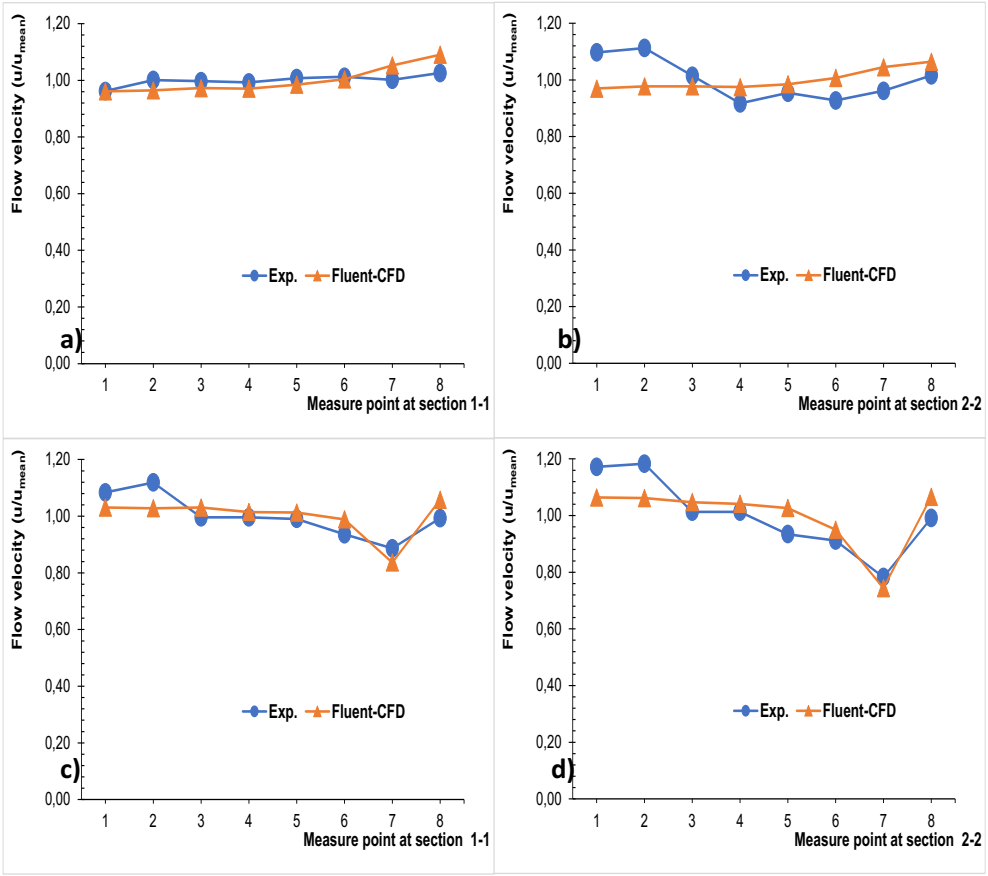


**Fig. 5.** ***Flow velocity changes for $V_0$ situation: a) Section 1-1, b) Section 2-2 and for $V_1$ situation: c) Section 1-1, d) Section 2-2***

The experimental and numerical model velocity values obtained in Section 1-1 are shown in Table 2 and Fig. 5c. When the table and graph are examined, it is seen that the error percentage of the velocities is less at the midpoints than at the edges. Maximum error was observed in the outer bank (2nd point) for $V_1$ situation 1-1 section (8%). According to Fig. 6c, decreases in flow velocities are seen behind the vane. Compared to the 1-1 section without the vane (Fig. 6c), it was observed that

the flow velocity decreased from 0.66 m/s to 0.46 m/s. It has been determined that there is a nearly 30% decrease in flow velocity. Also, as can be seen in Fig. 6c, the flow water depth in the inner bank and the water depth in the outer bank are balanced (the water depth changes with the blue contour lines). In general, it has been found that the test and CFD results are in good agreement.

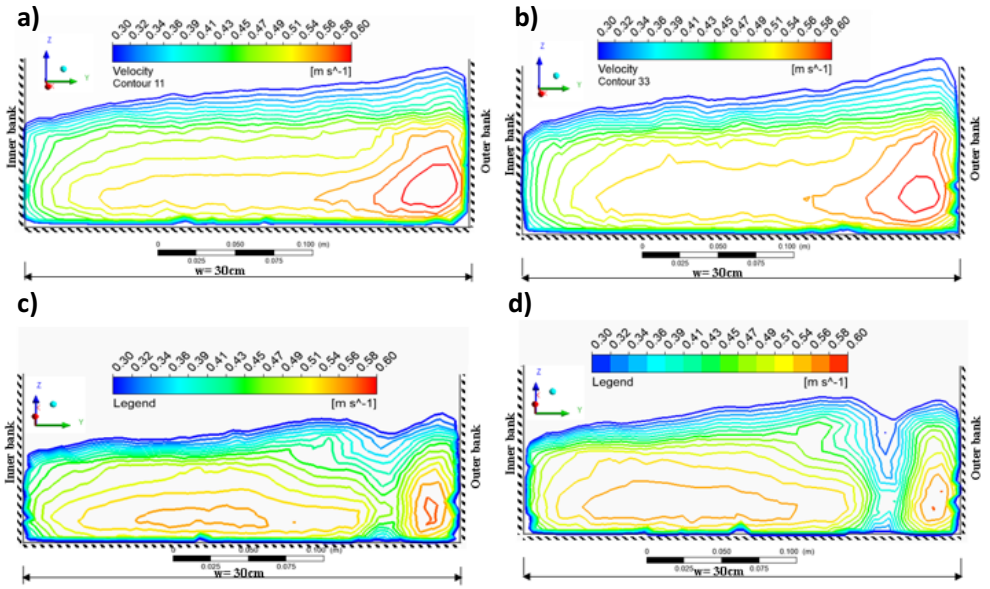


**Fig. 6.** ***Velocity value contours for Section 1-1 obtained as a result of CFD analysis***

The experimental and numerical model velocity values obtained in Section 2-2 are shown in Table 2 and Fig. 5d. Maximum error was observed in the inner bank (1-2 and 5th points) for $V_1$ situation 2-2 section (9-10%). In general, it has been found that the test and CFD results are in good agreement. According to Fig. 6d, decreases in flow velocities are seen behind the vane (as in section 1-1). Compared to the 2-2 section without the vane (Fig. 6b and 6d), it was observed that the flow velocity decreased from 0,65 m/s to 0,40 m/s. It has been determined that there is a nearly 38% decrease in flow rate. As can be seen in Fig. 6d, the flow water depth in the inner bank and the water depth in the outer bank are balanced. Considering the after-vane structure's measurements, the submerged vanes reduced a flow velocity of 30% in section 1-1 and decreased a flow velocity by 38% in section 2-2.

According to the $V_0$ and $V_1$ case, while the velocity decreases on the inner bank, velocity increases on the outer bank are observed. If the results of the experiments are examined in accordance with the CFD simulation results, a 12% error has been detected.

## 5. CONCLUSIONS

In this study, the performance of $V_0$ and $V_1$ situations a in open channel flows has been investigated by using a streamflow of 10 $L.s^{-1}$. The CFD streamflow

velocities were confirmed by experimental results of the flow velocities measured in the open channel flow. Effect of the vane structure on the flow velocity measured in the flow channel determined and the 2 cross-sectional velocity changes of the $V_1$ situation were compared experimentally and numerically each other's.

The simulated CFD velocity for the $V_0$ and $V_1$ were compared with the measured data. In order to see the amount of change, the measured and simulated flow velocity results are dimensionless based on the average velocity. It has been found that the experiment and numerical results give appropriate validation in $V_0$ and $V_1$ situations.

If the results of the experiments are examined in accordance with the CFD simulation results, a lower error has been detected. Within the scope of study, it was found that the submerged vanes significantly reduced the flow velocity when vane conditions were taken into account. It was found that 6 vane structures in single array affect the flow velocity by 30-38%. Submerged vane structures balance the streamflow water depth on the inner bank with the water depth on the outer bank within open channel flows.

## REFERENCES


1. Analysis Systems Inc., ANSYS fluent, Fluid Simulation software
2. Davoodi, L., & Bajestan, M. S. (2012). Control of sediment entry to intake on a trapezoidal channel by submerged vane. Ecology, Environment and Conservation, 18(1), 165-169.
3. Fathi, A., & Zomorodian, S. M. A. (2018). Effect of submerged vanes on scour around a bridge abutment. KSCE Journal of Civil Engineering, 22(7), 2281-2289.
4. Ghorbani, B., & Kells, J. A. (2008). Effect of submerged vanes on the scour occurring at a cylindrical pier. Journal of Hydraulic Research, 46(5), 610-619.
5. Hirt, C. W., & Nichols, B. D. (1981). Volume of fluid (VOF) method for the dynamics of free boundaries. Journal of Computational Physics, 39(1), 201–225. https://doi.org/10.1016/0021-9991(81)90145-5
6. Kalathil, S. T., Wuppukondur, A., Balakrishnan, R. K., & Chandra, V. (2018). Control of sediment inflow into a trapezoidal intake canal using submerged vanes. Journal of Waterway, Port, Coastal, and Ocean Engineering, 144(6), 04018020.
7. Lake, R. W., Shaeri, S., & Senevirathna, S. T. M. L. D. (2021). Design of submerged vane matrices to accompany a river intake in Australia. Journal of Environmental Engineering and Science, 16(2), 58-65.
8. Marelius, F., & Sinha, S. K. (1998). Experimental investigation of flow past submerged vanes. Journal of Hydraulic Engineering, 124(5), 542-545.
9. Odgaard, A. J., & Kennedy, J. F. (1982). Analysis of Sacramento River bend flows, and development of a new method for bank protection. IOWA INST OF HYDRAULIC RESEARCH IOWA CITY.
10. Odgaard, A. J., & Kennedy, J. F. (1983). River-bend bank protection by submerged vanes. Journal of Hydraulic Engineering, 109(8), 1161-1173.
11. Odgaard, A. J., & Lee, H. Y. E. (1984). Submerged vanes for flow control and bank protection in streams. Iowa Institute of Hydraulic Research, the University of Iowa.
12. Odgaard, A. J. (1987). Streambank erosion along two rivers in Iowa. Water Resources Research, 23(7), 1225-1236.

13. Üneş, F., & Varçin, H. (2017). 3-D real dam reservoir model for seasonal thermal density flow. *Environmental Engineering & Management Journal (EEMJ)*, *16*(9).